

## Coherent Submillimeter-Wave Emission from Bloch Oscillations in a Semiconductor Superlattice

Christian Waschke, Hartmut G. Roskos, Ralf Schwedler, Karl Leo, and Heinrich Kurz  
*Institut für Halbleitertechnik II, Rheinisch-Westfälische Technische Hochschule (RWTH) Aachen,  
 Sommerfeldstrasse 24, 5100 Aachen, Germany*

Klaus Köhler

*Fraunhofer-Institut für Angewandte Festkörperphysik, Tullastrasse 72, 7800 Freiburg, Germany*  
 (Received 22 January 1993)

We directly detect the coherent electromagnetic radiation originating from Bloch oscillations of charge carriers in an electrically biased semiconductor superlattice structure. The oscillation frequency can be tuned with the applied bias field from 0.5 THz to more than 2 THz, the detection limit of our measurement system.

PACS numbers: 73.20.Dx, 42.50.Md, 42.65.Re, 84.40.Cb

The work of Bloch on the dynamics of electron wave packets [1] in periodic potentials has led to the prediction [2] that an electron in uniform electric field  $F$  will undergo periodic oscillations with a frequency  $\nu_B = eFd/h$ , where  $d$  is the lattice constant and  $h$  denotes Planck's constant. These Bloch oscillations (BO) are caused by Bragg reflections of ballistically accelerated electrons at the Brillouin zone boundary. All attempts to observe BO in conventional bulk solids have failed. For all reasonable fields, the coherence of the Bloch states is destroyed by scattering before a single oscillation cycle is completed. In their pioneering work on semiconductor superlattices, Esaki and Tsu pointed out that BO of electrons should be observable in superlattices due to the high oscillation frequency expected even for modest fields [3]. They proposed BO as a source for tunable submillimeter-wave radiation. Subsequent theoretical work has shown that the quasiclassical theory is not adequate to describe BO [4–8]. It has to be replaced by a dynamical theory of wave packets composed of quasibound Wannier-Stark (WS) states. BO result from quantum beats of these states with the same oscillation period as that calculated with the quasiclassical model. Photocurrent and photoluminescence measurements on biased superlattices have proven the existence of the frequency-domain equivalent of BO, the WS ladder [9,10]. The simultaneous observation of WS states and the negative differential velocity [11] related to BO demonstrated the close relationship between WS localization and BO. Very recently, first evidence for BO in superlattices was found in degenerate four-wave-mixing experiments [12,13].

In this Letter, we directly prove the existence of BO by observing the submillimeter-wave emission from coherent charge carrier oscillations in a superlattice. We detect the electromagnetic “Bloch” radiation by using time-domain terahertz spectroscopy, a technique only sensitive to coherent emission processes [14]. The emission frequency can be tuned electrically from 0.5 THz up to the limit of our detection system above 2 THz.

The superlattice structure used in this study consists of

35 periods of nominally 34 monolayer (97 Å) thick GaAs well layers and 6 monolayer (17 Å) thick  $\text{Al}_{0.3}\text{Ga}_{0.7}\text{As}$  barrier layers. The undoped superlattice structure is grown by molecular beam epitaxy on an  $n$ -doped GaAs substrate with a 2500 Å thick undoped  $\text{Al}_{0.3}\text{Ga}_{0.7}\text{As}$  buffer layer beneath the superlattice region and a 3500 Å thick undoped  $\text{Al}_{0.3}\text{Ga}_{0.7}\text{As}$  buffer on top. A Kronig-Penney calculation gives a width of 19 meV (2 meV) for the lowest electron (heavy-hole) miniband. A reverse-bias field can be applied between the doped substrate and a semitransparent Cr Schottky contact on the sample surface. Increasing the bias from flatband conditions, one tunes the coupling between wells and with it the degree of localization of the electron and hole wave functions. At low reverse bias, close to flatband (0.6 V), strong interwell coupling leads to delocalization of the electron and hole wave functions over many superlattice periods [15] and to the formation of energy minibands. With increasing bias, the coupling between wells is gradually reduced: The wave functions are partly localized peaking in individual wells but extending into several neighboring wells [5]. Each energy miniband splits into a series of discrete levels forming a WS ladder as illustrated in the upper part of Fig. 1 [9,10,15]. For high reverse bias, the wave functions completely localize and the superlattice turns into a system of noninteracting multiple quantum wells [16].

To verify the formation of WS ladders in our sample, we have taken low-excitation photocurrent (PC) spectra at a temperature of 4 K. At low reverse bias, in the miniband regime from flatband up to about 0.0 V, the spectra are weakly structured. They reveal three delocalized exciton lines that we associate with the fundamental 1s heavy-hole (hh) excitons, the light-hole (lh) excitons, and excited hh excitons (hh2) marking the onset of the continuum [17]. At higher reverse bias, each line fans out into a series of discrete transitions as expected for hh and lh WS ladders. The lower part of Fig. 1 displays the energies of the detected excitonic interband transitions as a function of bias voltage. The WS transitions are la-

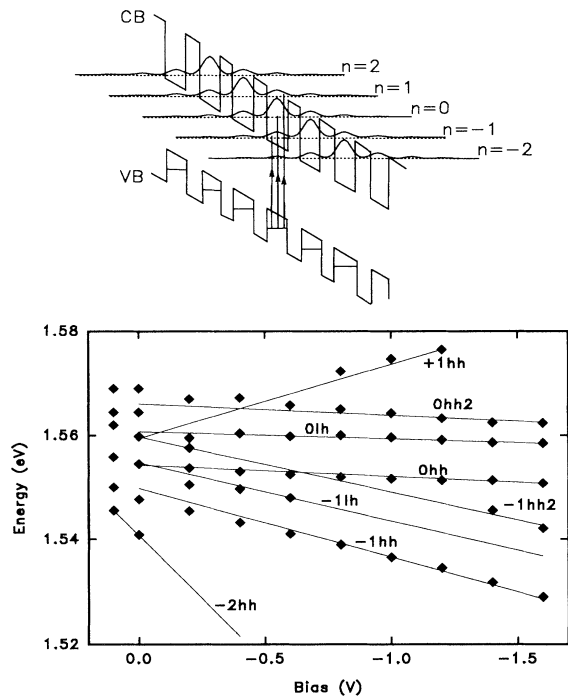


FIG. 1. Upper part: Schematic representation of the transitions from the valence band to the conduction band of a semiconductor superlattice in the Wannier-Stark bias regime. Lower part: Fan chart of the Wannier-Stark ladders as observed in PC spectra of our superlattice structure at  $T = 4$  K and at low excitation density.

beled by  $nhh$  and  $nlh$ , respectively. The index  $n$  denotes the position of the well where the final electron state is centered relative to the well where the hole probability density has its maximum value. In the PC spectra, we can distinguish  $hh$  transitions for  $n = -2, -1, 0$ , and  $+1$ , and  $lh$  transitions for  $n = -1$  and  $0$ , respectively. Around  $-1.6$  V, the WS regime starts to transform into the isolated-quantum-well regime with completely localized wave functions.

In the time-resolved experiment, we excite the sample by 100 fs optical pulses (bandwidth of 22 meV full width at half maximum) from a self-mode-locked Ti:sapphire laser. The wavelength (802 nm) is centered at the  $0hh$ -exciton transition. To detect the submillimeter-wave radiation from the sample in the time domain, we use a setup as described in Ref. [14]. The sample is mounted in a closed-cycle cryostat at a temperature of 15 K. An optical pulse incident under  $45^\circ$  generates excitons at a density below  $1 \times 10^9 \text{ cm}^{-2}$  per quantum well. Coherent THz radiation emitted nearly collinearly with the reflected optical beam leaves the cryostat through a silicon window (resistivity  $> 10 \text{ k}\Omega \text{ cm}$ ) and is projected via two off-axis paraboloidal mirrors onto a  $50\text{-}\mu\text{m}$  subpicosecond dipole antenna that is gated by a second, time-delayed part of the laser pulse.

The left part of Fig. 2 shows the detected coherent

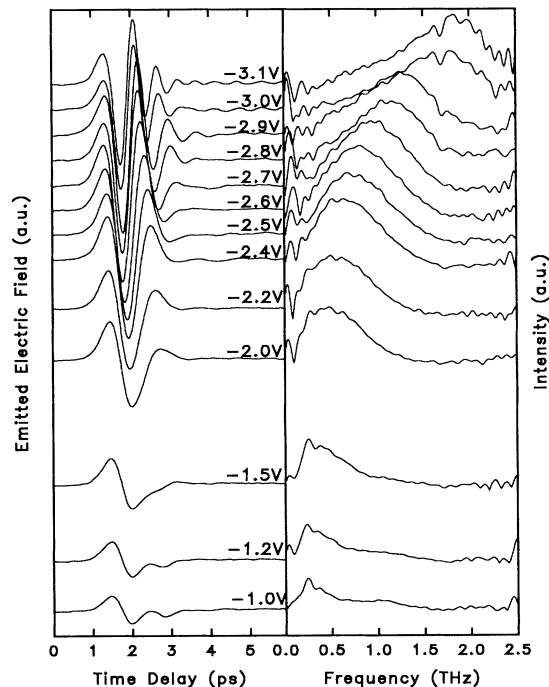


FIG. 2. Left side: Measured coherent electromagnetic transients emitted from the superlattice for different reverse-bias voltages. Right side: Fourier transforms of the time-domain data. The spectra are corrected for the frequency dependence of the detection system.

electromagnetic radiation as a function of time for different bias voltages. We distinguish two bias regimes, the reverse-bias domain from flatband ( $+0.6$  V) to  $-1.5$  V and the reverse-bias domain above  $-1.5$  V. Not shown are results close to flatband, where the THz-wave emission is rather weak and disappears completely at flatband. In Fig. 2, the THz-field amplitude increases continuously with voltage in the low-bias regime. Three oscillation cycles of the radiation are visible. The wave form hardly changes from flatband up to  $-1.0$  V. From  $-1.0$  V to  $-1.5$  V, the second maximum of the pulse begins to disappear. In the high-bias regime, above a reverse bias of  $-1.5$  V, we observe pronounced wave-form changes when the voltage is tuned. With rising bias, the number of detected oscillation cycles increases whereas the temporal spacing of the oscillation maxima continuously decreases. On the right side of Fig. 2, the Fourier spectra of the time-domain data are displayed. In the low-reverse-bias regime, the peak of the Fourier spectra is independent of the voltage. At high reverse bias, however, the peak of the Fourier spectra continuously shifts to higher frequency.

To relate the THz radiation to BO, we compare the Fourier spectra with PC and reflectance spectra of the sample. To avoid misinterpretations, it is *important to compare spectra that are taken under identical excitation conditions*: Even at the modest excitation of the

sample as in our THz-emission experiment, the onset of the WS ladder is shifted to higher bias voltages. The shift is caused by screening of the electric field across the superlattice by the accumulation of photogenerated charge carriers over many duty cycles of our 76 MHz laser system. We have verified that the charge carriers generated by a single optical pulse do not affect the screening of the electric field significantly. In the WS regime, the bias dependence of the transition energies does not change significantly (details will be published elsewhere).

To determine the origin of the tunable THz emission, we compare the data from time-resolved measurements with cw Wannier-Stark spectra taken under identical excitation conditions. We spectrally analyze the reflection of the laser beam used to excite THz emission. We record the reflectance change  $\Delta R$  induced by a slight modulation  $\Delta U = 0.2$  V of the bias voltage. Figure 3 shows electroreflectance spectra  $\Delta R/\Delta U$  for different bias voltages. Up to a reverse bias of  $-2.6$  V, the  $\Delta R/\Delta U$  spectra consist mainly of the bias derivative of two discrete lines separated by roughly 3.5 nm. This separation is expected between hh and lh excitons. For a reverse bias above  $-2.6$  V, three additional features emerge. They are marked in Fig. 3 by the dashed lines labeled  $-1hh$ ,  $-1lh$ , and  $-1hh2$ . With increasing bias, they gradually move towards longer wavelengths. The wavelength separation by 3.5 nm of the two features labeled  $-1hh$  and  $-1lh$  suggests that they correspond to hh and lh exciton

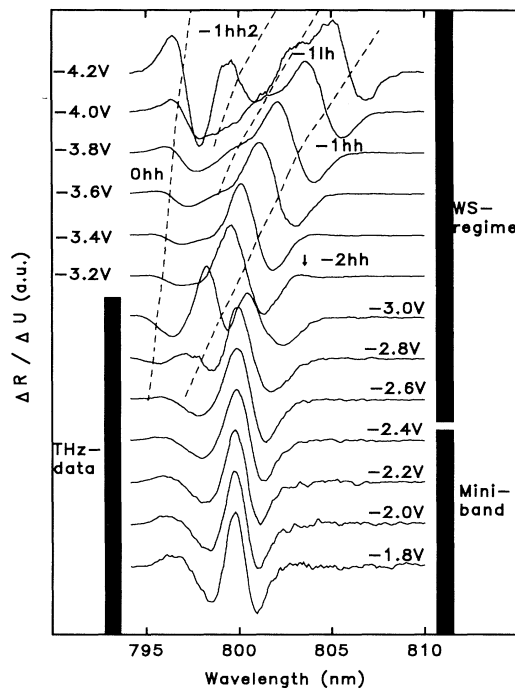


FIG. 3. Single-beam electroreflectance measurements of the superlattice sample for different bias voltages. The excitation conditions are identical to those of the THz-emission experiment.

transitions. Their bias dependence is identical to that of the  $-1hh$  and  $-1lh$  states in the PC spectra (Fig. 1); hence we identify the two features as  $-1hh$  and  $-1lh$  exciton transitions. The feature denoted by  $-1hh2$  has the same bias dependence as the  $-1hh$  and  $-1lh$  features. We assign it to higher exciton states at the onset of the continuum. The appearance of these three features above  $-2.6$  V obviously marks the onset of the WS regime at the excitation level of the THz-emission experiment. We can attribute the strong feature between 797 nm and 801 nm in the high-bias curves to the  $0hh$  transition. The weak feature at 803 nm in the  $-3.2$  V curve corresponds to a  $-2hh$  transition.

We now compare the THz-emission data with the results of the electroreflectance measurements: (i) The peak emission frequency depends weakly on the bias voltage for a reverse bias up to  $-2.5$  V where the reflectance spectra show the existence of a miniband regime. In this regime, the external bias voltage is quite effectively screened by accumulated charge carriers. (ii) The emission frequency depends linearly on voltage above  $-2.5$  V, where the reflectance spectra reveal the WS regime. In this bias range, the internal electric field is proportional to the external applied voltage. (iii) In the WS regime, the bias dependence of the emission frequency follows exactly the bias dependence of the energy separation between adjacent WS transitions. This is illustrated in Fig. 4. The full circles in Fig. 4 represent the photon energy  $h\nu_p$  of the THz transients. The open circles give the energy splitting  $\Delta E_{0,-1}$  between the  $0hh$  and  $-1hh$  tran-

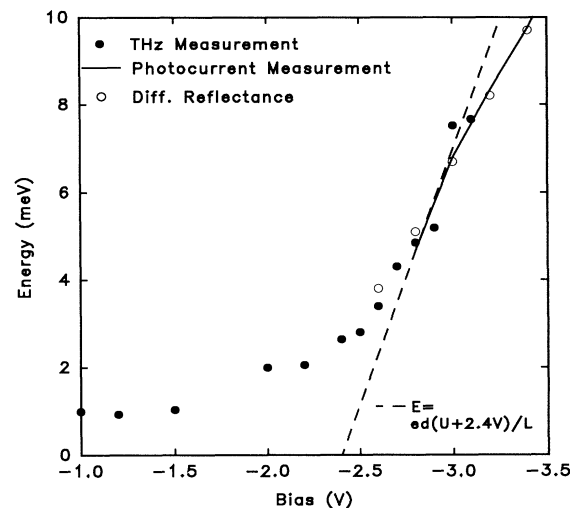


FIG. 4. Full circles: Photon energy of the THz radiation. Open circles: Energy separation of adjacent Wannier-Stark ladder states, extracted from the data of Fig. 3. Solid line: Energy separation of the  $n = -1$  and  $n = 0$  Wannier-Stark states in the PC spectra; the voltage of the PC data is shifted by an offset of  $-2.9$  V to account for field screening. Dashed line: Energy as calculated from simple BO theory as a function of the bias.

sitions in the electroreflectance measurement [18]. As shown in Fig. 4, the values of  $h\nu_p(U)$  and  $\Delta E_{0,-1}(U)$  overlap very well. (iv) The bias dependence of both  $h\nu_p$  and  $\Delta E_{0,-1}$  follows closely the bias dependence of the energy separation of adjacent WS transitions in the low-excitation PC spectra. This energy separation, extracted from the PC spectra of Fig. 1, is plotted as a solid line in Fig. 4. An offset of  $-2.9$  V has been added to the voltages of Fig. 1 to account for the shift of the WS regime by screening in the reflectance and THz-emission experiments. (v) The slope of  $h\nu_p$  and  $\Delta E_{0,-1}$  follows closely the relation  $\hbar\omega \sim edU/L$  expected from BO theory (see the dashed line in Fig 4). Here,  $d$  is the superlattice period and  $L$  the thickness of the electrically biased region.

We conclude from the comparison of the THz-emission spectra with the reflectance and PC spectra that the tunable THz radiation in the WS bias regime results from BO of the charge carriers after coherent excitation of several WS ladder transitions. In the THz-emission experiment, at least three WS transitions are excited (0hh,  $-1$ hh, and  $-2$ hh). It should be stressed that, from the wave-packet point of view, even the superposition of the wave functions of two WS states is sufficient to observe BO, i.e., an oscillation of the probability to find the WS wave packet at a given site with the time period  $eFd/h$  determined by the bias field  $F$  and the superlattice period  $d$ .

Our THz-emission data deviate in two aspects from the intuitive expectations for the THz emission of such a system: (i) Only in the regime where the WS ladder is visible in the reflectance spectra (above  $-2.5$  V), the frequency is linear with field as expected from the quasi-classical BO prediction. For lower bias fields, the photon energy increases sublinearly with bias. This observation qualitatively agrees with recent theoretical predictions [19] of a sublinear increase of the WS ladder energy  $eFd$  due to excitonic and Coulomb interaction. A quantitative comparison, however, is not possible since we cannot precisely relate the bias voltage  $U$  to the internal field  $F$  in this regime due to the screening effects. (ii) The THz-emission spectra (Fig. 2) do not show a strong broadband background signal [20] as has been observed in all other THz-emission experiments on semiconductor heterostructures (see, e.g., [14,21,22]). This observation will be the subject of further studies.

In summary, we have directly observed electromagnetic radiation from wave packets oscillating coherently in a semiconductor superlattice. In the Wannier-Stark bias regime, the electromagnetic radiation originates from Bloch oscillations of the charge carriers. Reflectance and four-wave-mixing measurements suggest that at high bias voltages THz radiation at frequencies as high as 5 THz may be generated. This remains to be verified with a THz measurement system with a larger detection bandwidth.

We are indebted to Jagdeep Shah for many stimulating

discussions. We thank P. Leisching and F. Brüggemann for their help with the screening studies, P. Haring Bolivar for the discussion of four-wave-mixing results, and H. Bakker, S. L. Chuang, G. Bastard, P. Voisin, M. Luban, and A. Bouchard for helpful comments. This work has been supported by the Volkswagen-Stiftung.

- 
- [1] F. Bloch, Z. Phys. **52**, 555 (1928).
  - [2] C. Zener, Proc. R. Soc. London Ser. A **145**, 523 (1934).
  - [3] L. Esaki and R. Tsu, IBM J. Res. Dev. **14**, 61 (1970).
  - [4] J. B. Krieger and G. J. Iafrate, Phys. Rev. B **33**, 5494 (1986).
  - [5] G. Bastard and R. Ferreira, in *Spectroscopy of Semiconductor Microstructures*, NATO ASI Series (Plenum, New York, 1989), p. 333.
  - [6] A. M. Bouchard and M. Luban, Phys. Rev. B **47**, 6815 (1993).
  - [7] G. von Plessen and P. Thomas, Phys. Rev. B **45**, 9185 (1992).
  - [8] G. Bastard and R. Ferreira, C. R. Acad. Sci. Paris **312**, 971 (1991).
  - [9] J. Bleuse, G. Bastard, and P. Voisin, Phys. Rev. Lett. **60**, 220 (1988).
  - [10] E. E. Mendez, F. Agulló-Rueda, and J. M. Hong, Phys. Rev. Lett. **60**, 2426 (1988).
  - [11] A. Sibille, J. F. Palmier, and F. Molloy, Appl. Phys. Lett. **60**, 457 (1992).
  - [12] J. Feldmann, K. Leo, J. Shah, D. A. B. Miller, J. E. Cunningham, T. Meier, G. von Plessen, A. Schulze, P. Thomas, and S. Schmitt-Rink, Phys. Rev. B **46**, 7252 (1992).
  - [13] K. Leo, P. Haring Bolivar, F. Brüggemann, R. Schwedler, and K. Köhler, Solid State Commun. **84**, 943 (1992).
  - [14] H. G. Roskos, M. C. Nuss, J. Shah, K. Leo, D. A. B. Miller, A. M. Fox, S. Schmitt-Rink, and K. Köhler, Phys. Rev. Lett. **68**, 2216 (1992).
  - [15] F. Agulló-Rueda, E. E. Mendez, and J. M. Hong, Phys. Rev. B **40**, 1357 (1989).
  - [16] In superlattices with low miniband width, excitonic effects suppress the formation of a Wannier-Stark ladder. The miniband regime then directly transforms to the isolated-quantum-well regime [A. M. Fox, D. A. B. Miller, J. E. Cunningham, W. Y. Jan, C. Y. P. Chao, and S. L. Chuang, Phys. Rev. B **46**, 15365 (1992)].
  - [17] F. Agulló-Rueda, J. A. Brum, E. E. Mendez, and J. M. Hong, Phys. Rev. B **41**, 1676 (1990).
  - [18] The data points used for this analysis are located on the dashed lines of Fig. 3 denoted by 0hh and  $-1$ hh.
  - [19] M. M. Dignam and J. E. Sipe, Phys. Rev. B **43**, 4097 (1991).
  - [20] S. L. Chuang, S. Schmitt-Rink, B. I. Greene, P. N. Saeta, and A. F. J. Levi, Phys. Rev. Lett. **68**, 102 (1992).
  - [21] P. C. M. Planken, M. C. Nuss, W. H. Knox, D. A. B. Miller, and K. W. Goossen, Appl. Phys. Lett. **61**, 2009 (1992).
  - [22] P. C. M. Planken, M. C. Nuss, I. Brener, K. W. Goossen, M. S. C. Luo, S. L. Chuang, and L. Pfeiffer, Phys. Rev. Lett. **69**, 3800 (1992).